

Design and Implementation of a Takum Arithmetic Hardware Codec

Laslo Hunhold 

Parallel and Distributed Systems Group
University of Cologne, Cologne, Germany
hunhold@uni-koeln.de

Abstract The takum machine number format has been recently proposed as an enhancement over the posit number format, which is considered a promising alternative to the IEEE 754 floating-point standard. Takums retain the useful posit properties, but feature a novel exponent coding scheme that yields more precision for small and large magnitude numbers and a much higher and bounded dynamic range.

This paper presents the design and implementation of a hardware codec for both takums (logarithmic number system, LNS) and linear takums (floating-point format). The codec design is emphasised, as it constitutes the primary distinguishing feature compared to logarithmic posits (LNS) and posits (floating-point format), which otherwise share similar internal representations. Furthermore, a novel internal representation for LNS is proposed. The presented takum codec, implemented in VHDL, demonstrates near-optimal scalability and performance on an FPGA. It achieves latency reductions of up to 38 % and reduces LUT utilisation up to 50 % compared to the best state-of-the-art posit codecs.

Keywords: machine numbers · takum arithmetic · posit arithmetic · logarithmic number system · floating-point arithmetic · HDL · VHDL · FPGA

1 Introduction

For decades, IEEE 754 floating-point numbers have been the dominant format for representing real numbers in computing. However, recent demands for low- and mixed-precision arithmetic in fields such as machine learning have highlighted significant shortcomings of the IEEE 754 standard, particularly in terms of reproducibility, precision and dynamic range. While modifications within the IEEE 754 framework, such as Google’s `bfloat16` [19], have been proposed to address these issues, more fundamental changes to computer arithmetic are also being explored. One such innovation is posit arithmetic [5, 6], which has garnered significant attention in recent years. Posits have *tapered precision* by encoding the exponent with variable length, allowing for more fraction bits around numbers near 1, at the expense of fewer fraction bits for numbers of very small or large magnitude. This encoding also allows treating posits like two’s complement integers in terms of sign, ordering and negation.

The posit format is generally considered simpler to implement in hardware compared to IEEE 754 floating-point numbers, largely due to the reduction of special cases. Over the past few years, several optimised hardware implementations have been developed. Initial work is documented in [2, 18], with further optimisations leading to the creation of the FloPoCo posit core generator [14, 16, 15, 13]. This culminated in the development of a complete RISC-V posit core supporting up to 64-bit precision [12, 11]. Despite the potential of posits in various low- and mixed-precision applications [1, 17], several challenges have hindered their adoption. Chief among these is the sharp decline in precision for small and large magnitude numbers and the lack of dynamic range, which poses significant problems for general-purpose arithmetic applications and numerical methods [3, 7].

In response to these challenges, the takum format was recently proposed [7]. Takum introduces a new encoding scheme that guarantees a minimum of $n - 12$ fraction bits and achieves a significantly increased dynamic range that is fully realised at 12-bit precision, remaining constant thereafter. This design not only makes takums suitable for applying well-established numerical analysis techniques, but it also decouples the choice of precision from dynamic range concerns in mixed-precision applications. This property is reflected in its name, derived from the Icelandic ‘*takmarkað umfang*’, meaning ‘limited range’.

While the takum format has been formally verified [7], its hardware implementation has only been briefly touched upon in [7, Section 5.2], with claims that it should be simpler than posit implementations. The primary reason is that the takum exponent is at most 11 bits long, as opposed to potentially occupying the entire width, as is the case with posits. Consequently, the bit string length in takum should have minimal impact on the complexity of encoding and decoding processes, unlike in posit arithmetic. However, the upfront computational costs of takum encoding and decoding remain an open question.

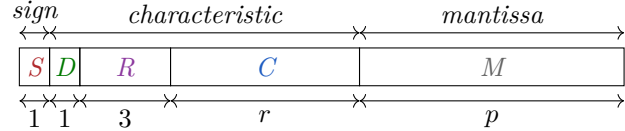
This paper makes three primary contributions: (1) it derives efficient algorithms for encoding and decoding takum numbers, proposing a new logarithmic number system (LNS) internal representation; (2) it provides a detailed open-source VHDL implementation optimised for but not limited to FPGA hardware; and (3) it compares the performance of the takum codec with state-of-the-art posit codecs.

The remainder of this paper is organised as follows: Section 2 defines the takum format in both its logarithmic and linear forms. Section 3 introduces a novel internal representation for logarithmic number systems, inspired by recent advances in posit codecs. Sections 4 and 5 then detail the design and implementation of a takum decoder and encoder, respectively. Section 6 presents an evaluation of the VHDL implementation on FPGA, followed by a conclusion and outlook in Section 7.

2 Takum Encoding Scheme

We begin by defining the (logarithmic) takum encoding scheme, originally introduced in [7], as its binary format and notation will be extensively referenced throughout this work. In terms of notation, for a bit string $B \in \{0, 1\}^n$, \bar{B} denotes its complement.

Definition 1 (takum encoding [7, Definition 2]). Let $n \in \mathbb{N}$ with $n \geq 12$. Any n -bit MSB \rightarrow LSB string $T := (\textcolor{red}{S}, \textcolor{green}{D}, \textcolor{purple}{R}, \textcolor{blue}{C}, M) \in \{0, 1\}^n$ of the form



with sign bit $\textcolor{red}{S}$, direction bit $\textcolor{green}{D}$, regime bits $\textcolor{purple}{R} := (\textcolor{purple}{R}_2, \textcolor{purple}{R}_1, \textcolor{purple}{R}_0)$, characteristic bits $\textcolor{blue}{C} := (\textcolor{blue}{C}_{r-1}, \dots, \textcolor{blue}{C}_0)$, mantissa bits $M := (M_{p-1}, \dots, M_0)$, regime

$$r := \begin{cases} \text{uint}(\bar{\textcolor{purple}{R}}) & \textcolor{green}{D} = 0 \\ \text{uint}(\textcolor{purple}{R}) & \textcolor{green}{D} = 1 \end{cases} \in \{0, \dots, 7\}, \quad (1)$$

characteristic

$$c := \begin{cases} -2^{r+1} + 1 + \text{uint}(\textcolor{blue}{C}) & \textcolor{green}{D} = 0 \\ 2^r - 1 + \text{uint}(\textcolor{blue}{C}) & \textcolor{green}{D} = 1 \end{cases} \in \{-255, \dots, 254\}, \quad (2)$$

mantissa bit count $p := n - r - 5 \in \{n - 12, \dots, n - 5\}$, mantissa $m := 2^{-p} \text{uint}(M) \in [0, 1)$ and logarithmic value

$$\ell := (-1)^{\textcolor{red}{S}} (c + m) \in (-255, 255) \quad (3)$$

encodes the takum value

$$\tau(T) := \begin{cases} 0 & \textcolor{red}{S} = 0 \\ \text{NaR} & \textcolor{red}{S} = 1 \quad \textcolor{green}{D} = \textcolor{purple}{R} = \textcolor{blue}{C} = M = \mathbf{0} \\ (-1)^{\textcolor{red}{S}} \sqrt{e}^\ell & \text{otherwise} \end{cases} \quad (4)$$

with $\tau: \{0, 1\}^n \mapsto \{0, \text{NaR}\} \cup \pm (\sqrt{e}^{-255}, \sqrt{e}^{255})$ and EULER's number $e \approx 2.718$ (and thus $\sqrt{e} \approx 1.649$). Any bit string shorter than 12 bits is also considered in the definition by assuming the missing bits to be zero bits ('ghost bits').

Takums are uniformly defined for arbitrary bit-string lengths n , unlike IEEE 754 floating-point numbers, which are only non-uniformly defined for specific values of n . Although takums are primarily defined as an LNS, linear takums, their floating-point variant, retain a structure that closely mirrors the original LNS format.

Definition 2 (linear takum encoding [7, Definition 20]). Take Definition 1 and rename the mantissa bit count p , mantissa bits M and mantissa m to fraction bit count p , fraction bits F and fraction f . Define the exponent

$$e := (-1)^{\textcolor{red}{S}}(c + \textcolor{red}{S}) \in \{-255, \dots, 254\} \quad (5)$$

and the linear takum value encoding as

$$\bar{\tau}(T) := \begin{cases} 0 & \textcolor{red}{S} = 0 \\ \text{NaR} & \textcolor{red}{S} = 1 \\ [(1 - 3\textcolor{red}{S}) + f] \cdot 2^e & \text{otherwise.} \end{cases} \quad \textcolor{green}{D} = \textcolor{violet}{R} = \textcolor{blue}{C} = F = \mathbf{0} \quad (6)$$

As we can see, both the logarithmic and linear definitions of takum are largely similar. In this paper, we will adhere closely to both definitions for the development of the codec. Please refer to [7] for an overview of the numerical properties.

3 Internal Representations

While it is clear that the decoder's input, as well as the encoder's output, is a binary representation of a takum, defining the decoder's output and encoder's input in general cases is more complex. This internal representation must not only uniquely identify a takum but also facilitate efficient arithmetic operations. Typically, decoders and encoders are used as input and output stages within an arithmetic unit, so the internal representation should be optimised for these contexts. In general, special cases (zero and NaR) are represented separately; thus, the following discussion of internal representations pertains only to non-zero real numbers.

In the linear case, the most straightforward approach would be to use the standard floating-point internal representation of the form

$$(\textcolor{red}{S}, \hat{e}, \hat{f}) \mapsto (-1)^{\textcolor{red}{S}} (1 + \hat{f}) \cdot 2^{\hat{e}} \quad (7)$$

with $\hat{f} \in [0, 1)$ and $\hat{e} \in \{-254, \dots, 254\}$. However, as demonstrated by Yonemoto [5] for the default internal representation of posits and further generalised by [13], it is more effective to adopt the internal representation

$$(\textcolor{red}{S}, e, f) \mapsto [(1 - 3\textcolor{red}{S}) + f] \cdot 2^e \quad (8)$$

with $f \in [0, 1)$ and $e \in \{-255, \dots, 254\}$. This choice is advantageous because the internal representation is monotonic in f , similar to how the fraction bits F are monotonic in takum encoding. This monotonicity avoids the need for a full two's complement negation of the fraction during decoding and encoding when $\textcolor{red}{S}$ is 1, as would be necessary with the representation in (7). The trade-off between (7) and (8) involves a slightly more complex arithmetic for the latter and a departure from the extensive body of work associated with the former, as discussed in [15, 13]. Moreover, examining the exponent definition, $e = (-1)^{\textcolor{red}{S}}(c + \textcolor{red}{S})$, reveals that

it simplifies to c when $\textcolor{red}{S} = 0$, and to the bitwise complement of c , assuming c is represented as a two's complement integer, when $\textcolor{red}{S} = 1$.

Turning to the logarithmic case, the canonical internal representation is given by

$$(\textcolor{red}{S}, \ell) \mapsto (-1)^{\textcolor{red}{S}} \sqrt{e}^\ell \quad (9)$$

where $\ell \in (-255, 255)$. This representation is also utilised in the most recent work on logarithmic posits [17]. However, this approach has a drawback similar to the linear case, as it necessitates a two's complement negation both after decoding to and before encoding from the internal representation. By definition, $\ell = (-1)^{\textcolor{red}{S}}(c + m)$. An alternative we propose here is to define a ‘barred logarithmic value’ as $\bar{\ell} := c + m = (-1)^{\textcolor{red}{S}}\ell \in (-255, 255)$ and use the internal representation

$$(\textcolor{red}{S}, \bar{\ell}) \mapsto (-1)^{\textcolor{red}{S}} \sqrt{e}^{(-1)^{\textcolor{red}{S}}\bar{\ell}}. \quad (10)$$

The advantage of this novel representation is that $\bar{\ell}$ is monotonic in m , just as the mantissa bits M are monotonic in takum encoding. This monotonicity eliminates the need for two's complement negations after decoding and before encoding. The impact on arithmetic complexity is minimal, as all sign cases of ℓ must be handled regardless. For instance, when computing the square root, which involves a right shift of ℓ , the procedure remains unchanged. Similarly, multiplication and division require handling all sign combinations of ℓ , as does addition and subtraction.

The barred logarithmic value $\bar{\ell}$ can be easily derived from c and m by concatenating the 9-bit signed integer c with the $(n - 5)$ -bit unsigned integer $2^{n-5} \cdot m$ (given $p+r = n-5$), which is then interpreted as an $(n+4)$ -bit fixed-point number. In general, whether in the linear or logarithmic case, the internal representations $(\textcolor{red}{S}, e, f)$ and $(\textcolor{red}{S}, \bar{\ell})$ are straightforward to determine from the characteristic c and the equivalent fraction f and mantissa m .

4 Decoder

The purpose of the decoder is to transform a given n -bit takum binary representation, where $n \in \mathbb{N}_2$ (the set of natural numbers greater than or equal to 2), into its corresponding internal representation. Specifically, this internal representation is expressed as $(\textcolor{red}{S}, e, f)$ in the linear case and as $(\textcolor{red}{S}, \bar{\ell})$ in the logarithmic case (see (8) and (10)). As demonstrated in Section 3, both forms of internal representation can be directly derived from the characteristic c and the mantissa m (where the fraction f corresponds to m). Consequently, our primary objective is to determine c and m , as they serve as the common foundation for both cases to derive the respective internal representation. Additionally, if the input corresponds to 0 or NaR, this should also be appropriately flagged.

Given that takums are a tapered precision machine number format, it is also essential to determine the number of mantissa bits (precision) for a given input. The direction bit $\textcolor{blue}{D}$ (*direction_bit*) and the sign bit $\textcolor{red}{S}$ (*sign*) can be

straightforwardly extracted from the two most significant bits (MSBs) of the input.

4.1 Characteristic/Exponent Determinator

To determine the characteristic (and later, the exponent), we focus on the following problem reduction: Referring to the takum bit pattern defined in Definition 1 and considering that both the characteristic length and the bit pattern are variable, it is most effective to expand the bit pattern to 12 bits and then extract the 7 bits that follow the regime. This extraction will be carried out later; our current focus is on the processing of these bits. These 7 bits, which we refer to as the raw characteristic (*characteristic_raw_bits*), are guaranteed to include all *regime* characteristic bits, followed by $7 - \text{regime} =: \text{antiregime}$ waste bits.

If we examine the definition of the characteristic provided in (2), we observe that it involves introducing a bias to the characteristic bits. This process entails a bitwise operation, followed by either an increment or a decrement of the bits. To simplify the procedure and avoid the need for decrements, we propose a normalisation approach that exclusively relies on increments. To justify this approach, we first present the following

Proposition 1 (characteristic complement). *Let $n \in \mathbb{N}_1$ and bit string $T := (\textcolor{red}{S}, \textcolor{green}{D}, \textcolor{purple}{R}, \textcolor{blue}{C}, M) \in \{0, 1\}^n$ as in Definition 1 with $\tau((\textcolor{red}{S}, \textcolor{green}{D}, \textcolor{purple}{R}, \textcolor{blue}{C}, M)) \notin \{0, \text{NaR}\}$, characteristic c and regime r . Let $\tilde{T} := (\tilde{\textcolor{red}{S}}, \tilde{\textcolor{green}{D}}, \tilde{\textcolor{purple}{R}}, \tilde{\textcolor{blue}{C}}, \tilde{M}) \in \{0, 1\}^n$ with characteristic \tilde{c} , regime \tilde{r} and arbitrary $\tilde{\textcolor{red}{S}}$ and \tilde{M} . It holds $\tilde{r} = r$ and $\tilde{c} = -c - 1$. This means that, assuming c is represented as a two's complement integer, \tilde{c} is obtained directly as the bitwise complement of c .*

Proof. It follows by definition that $\tilde{r} = r$ given the complementation of the direction bit cancels out that of the regime bits, yielding the same regime value. It holds for the characteristic value

$$\tilde{c} = \sum_{i=0}^{r-1} \textcolor{blue}{C}_i 2^i + \begin{cases} -2^{r+1} + 1 & \textcolor{green}{D} = 0 \\ 2^r - 1 & \textcolor{green}{D} = 1 \end{cases} \quad (11)$$

$$= (2^r - 1) - \sum_{i=0}^{r-1} \textcolor{blue}{C}_i 2^i + \begin{cases} -2^{r+1} + 1 & \textcolor{green}{D} = 0 \\ 2^r - 1 & \textcolor{green}{D} = 1 \end{cases} \quad (12)$$

$$= - \left(\sum_{i=0}^{r-1} \textcolor{blue}{C}_i 2^i + \begin{cases} 2^r - 1 & \textcolor{green}{D} = 0 \\ -2^{r+1} + 1 & \textcolor{green}{D} = 1 \end{cases} \right) - 1 \quad (13)$$

$$= -c - 1. \quad (14)$$

Thus we have proven what was to be shown. \square

As observed, negating the direction bit, the regime bits, and the characteristic bits corresponds to negating the characteristic value, which is represented in two's complement. This property can be leveraged in the following manner:

Table 1: All possible biases -2^{r+1} given as 9-bit two's complement integers for all regimes r ranging from 0 to 7. The r least significant bits are underlined.

r	-2^{r+1}	r	-2^{r+1}
0	11111110	4	1111 <u>00000</u>
1	111111 <u>100</u>	5	111 <u>0000000</u>
2	11111 <u>1000</u>	6	11 <u>00000000</u>
3	<u>111110000</u>	7	1 <u>000000000</u>

Corollary 1 (conditional characteristic complement). Let $n \in \mathbb{N}_1$ and $T := (\textcolor{red}{S}, \textcolor{green}{D}, \textcolor{purple}{R}, \textcolor{blue}{C}, M) \in \{0, 1\}^n$ as in Definition 1 with $\tau((\textcolor{red}{S}, \textcolor{green}{D}, \textcolor{purple}{R}, \textcolor{blue}{C}, M)) \notin \{0, \text{NaR}\}$, characteristic c and regime r . Let

$$\tilde{T} := \begin{cases} (\textcolor{red}{S}, \textcolor{green}{D}, \textcolor{purple}{R}, \textcolor{blue}{C}, M) & \textcolor{green}{D} = 0 \\ (\textcolor{red}{S}, \overline{\textcolor{green}{D}}, \overline{\textcolor{purple}{R}}, \overline{\textcolor{blue}{C}}, M) & \textcolor{green}{D} = 1 \end{cases} \quad (15)$$

with characteristic \tilde{c} and regime \tilde{r} . It holds $\tilde{r} = r$ and

$$\tilde{c} = \begin{cases} c & \textcolor{green}{D} = 0 \\ -c - 1 & \textcolor{green}{D} = 1 \end{cases} = \begin{cases} -2^{r+1} + 1 + \sum_{i=0}^{r-1} \textcolor{blue}{C}_i 2^i & \textcolor{green}{D} = 0 \\ -2^{r+1} + 1 + \sum_{i=0}^{r-1} \overline{\textcolor{blue}{C}}_i 2^i & \textcolor{green}{D} = 1. \end{cases} \quad (16)$$

It should be noted that c can be obtained from $-c - 1$ by a simple bitwise complement, assuming c is represented as a two's complement integer.

Proof. This follows directly from Proposition 1 and Definition 1. \square

This approach suggests a strategy for determining the characteristic c : First, conditionally negate the characteristic bits when the direction bit is 1. Next, apply the bias -2^{r+1} unconditionally, then increment the result. Finally, conditionally negate the intermediate result \tilde{c} when the direction bit is 1 to obtain the final characteristic c . This ensures that the process involves only incrementing in all cases (without any decrement), allowing us to focus solely on the single application of the bias -2^{r+1} .

Fortunately, the application of the bias is straightforward: As illustrated in Table 1, each of the 8 possible biases can be added to the r characteristic bits, assuming they are represented as a two's complement integer, using a simple bitwise OR operation. Additionally, since the $(r + 1)$ th bit is always zero in the biases, the bias can also be applied using a bitwise OR operation on the incremented characteristic bits.

However, we adopt a different approach: Given that our raw characteristic contains the left-aligned characteristic bits, we first invert these bits if the direction bit is 1. Next, we prepend the bits 10 to the left and perform an *arithmetic* right shift by the *antiregime* bits. This process yields the desired bitwise OR of the bias with the characteristic bits. Subsequently, we increment the first 8 bits

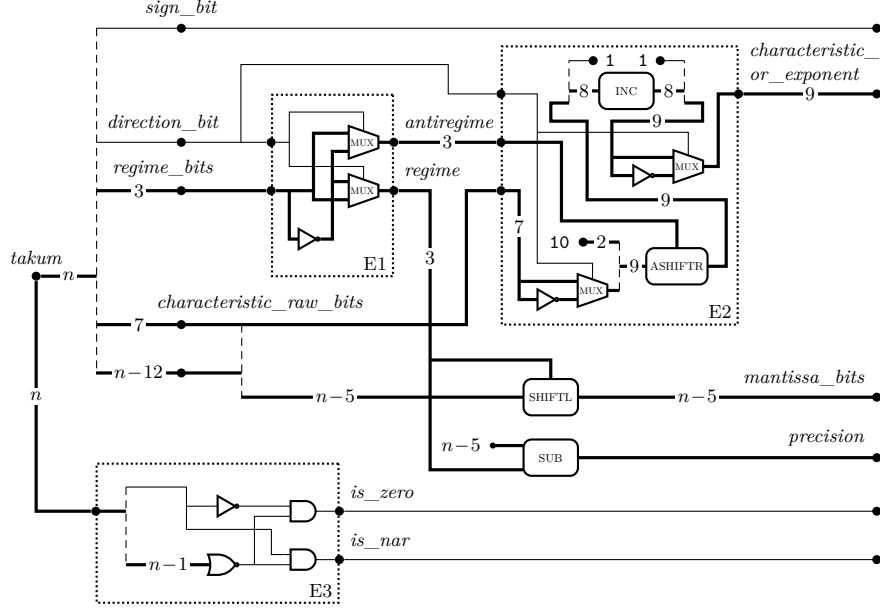


Figure 1: The logic circuit of the predecoder, largely separated into three main entities: the regime/antiregime determinator (E1), the characteristic/exponent determinator (E2) and the special case detector (E3). We assume $n \geq 12$ (thus omitting optional zero-expansion of *takum* at the beginning for $n < 12$) for simplicity; the implemented predecoder works for any $n \geq 2$. We also assume an enabled *output_exponent*, as disabling it would only flip the top MUX in E2. Vertical dashed lines indicate where the strands of a multi-signal are split up or combined.

of the resulting value, prepend 1 to the left, and then conditionally negate the outcome based on the direction bit, as illustrated in Corollary 1.

Referring back to the previously discussed internal representations in Section 3, it was noted that in the case of linear takums, the exponent is obtained by negating the characteristic. Rather than performing this negation separately, which would introduce additional overhead, we introduce an additional input bit, *output_exponent*. This parameter, which is set during synthesis and not a true input bit of the entity, inverts the conditional negation we already perform, thus providing the exponent negation at no extra cost.

4.2 Pre-, Logarithmic and Linear Decoder

We integrate the characteristic/exponent determinator into the predecoder to determine the sign, characteristic or exponent (depending on *output_exponent*), and mantissa. Both parameters n and *output_exponent* are already set during

synthesis, thereby eliminating many conditional operations. In total the pre-decoder is made up of three entities: the regime/antiregime determinator (E1), the previously described characteristic/exponent determinator (E2) and the special cases detector (E3) [8, rtl/decoder/predecoder.vhd, lines 74–133]. A full logic circuit is outlined in Figure 1.

For the decoding of logarithmic takums the predecoder output is utilised to concatenate the characteristic and mantissa, forming the barred logarithmic value as defined in (10) [8, rtl/decoder/decoder_logarithmic.vhd]. The linear decoder, detailed in [8, rtl/decoder/decoder_linear.vhd], leverages the predecoder to produce the internal representation described by (8). In this context, the input bit parameter *output_exponent* is set to 1 within the predecoder to directly yield the exponent instead of the characteristic.

5 Encoder

The objective of the encoder is to transform a given internal representation into the takum binary representation for a specified $n \in \mathbb{N}_2$. The internal representation is given by (S, e, f) in the linear case and by $(S, \bar{\ell})$ in the logarithmic case, as defined in (8) and (10), respectively.

As discussed in Section 3, both internal representations can be readily converted into the characteristic c and the mantissa m (where the fraction f corresponds to m). Therefore, we can consider both representations as equivalent starting points for either case. The direction bit D (denoted as *direction_bit*) can be straightforwardly determined by noting that it takes the value 1 when the characteristic satisfies $characteristic \geq 0$.

5.1 Underflow/Overflow Predictor

Early in the process, it is crucial to predict whether the value we intend to encode might result in either an underflow or overflow, particularly since we are adhering to sticky arithmetic. In sticky arithmetic, such under- or overflows do not yield zero or infinity, but instead saturate at the smallest or largest representable number, respectively. Anticipating these potential outcomes early on enables us to significantly reduce the time on the critical path, as opposed to the alternative method of unconditionally rounding at the end and subsequently checking for overflow or underflow.

To predict rounding, we can differentiate between two distinct cases that are both handled in the encoder. The first case occurs when n lies between 2 and 11. In this scenario, the rounding boundary is positioned within the regime or characteristic. As detailed in Table 2, we can see that under- and overflow can be predicted with the given characteristic.

The second scenario considers the case where $n \geq 12$. By construction, it is evident that a necessary condition for underflow when rounding down and overflow when rounding up occurs when the first 12 bits take the forms **X000000000000** and **X1111111111** respectively. This is because the direction bit and the regime

Table 2: Bit pattern and subsequent characteristic bounds where rounding down would underflow to zero or rounding up would overflow to NaR for the special cases $n \in \{2, \dots, 11\}$. The rounding boundary is indicated with a small gap.

n	round-down underflows \leq	$c \leq$	round-up overflows \geq	$c \geq$
2	X0 1111...1	-1	X1 0000...0	0
3	X00 111111...1	-16	X11 000000000...0	15
4	X000 1111111...1	-64	X111 00000000...0	63
5	X0000 11111111...1	-128	X1111 00000000...0	127
6	X00000 1111111...1	-192	X11111 0000000...0	191
7	X000000 111111...1	-224	X111111 000000...0	223
8	X0000000 111111...1	-240	X1111111 00000...0	239
9	X00000000 1111...1	-248	X11111111 0000...0	247
10	X000000000 111...1	-252	X111111111 000...0	251
11	X0000000000 11...1	-254	X1111111111 00...0	253

bits being all zeros or all ones directly imply that the regime value is 7. Consequently, in the overflow scenario, the necessary condition $c = -255$ or $c = 254$ is satisfied.

To establish a sufficient condition for underflow or overflow, we must examine the mantissa bits. For underflow, these bits must be all zeros, and for overflow, they must be all ones, up to and including the most significant rounding bit, which is consistently positioned since the regime value is always 7. Given that the bits preceding the mantissa have a fixed length of 12, we need to inspect the $n - 11$ most significant mantissa bits. When rounding down would result in underflow or rounding up would lead to overflow, an output signal is generated to indicate the respective condition for later usage in the encoder by the rounder [8, rtl/encoder/postencoder.vhd, lines 33–107].

5.2 Characteristic Precursor Determinator

The initial step in the encoding process involves determining the regime and characteristic bits from the given characteristic. To facilitate this, the characteristic is first normalised into a format that allows for the efficient extraction of both the regime and characteristic bits, regardless of the scenario. We refer to this specific format as the ‘characteristic precursor’. The characteristic precursor can be derived using the following

Proposition 2 (characteristic precursor). *Let $n \in \mathbb{N}_1$ and bit string $T := (\textcolor{red}{S}, \textcolor{green}{D}, \textcolor{purple}{R}, \textcolor{blue}{C}, \textcolor{brown}{M}) \in \{0, 1\}^n$ as in Definition 1 with $\tau((\textcolor{red}{S}, \textcolor{green}{D}, \textcolor{purple}{R}, \textcolor{blue}{C}, \textcolor{brown}{M})) \notin \{0, \text{NaR}\}$, two’s complement characteristic c and regime r . It holds*

$$\begin{cases} -c - 1 & \textcolor{green}{D} = 0 \\ c & \textcolor{green}{D} = 1 \end{cases} + 1 = \begin{cases} 2^r + \sum_{i=0}^{r-1} \textcolor{blue}{C}_i 2^i & \textcolor{green}{D} = 0 \\ 2^r + \sum_{i=0}^{r-1} \textcolor{blue}{C}_i 2^i & \textcolor{green}{D} = 1. \end{cases} \quad (17)$$

It should be noted that $-c - 1$ can be obtained from c by a simple bitwise complement, assuming c is represented as a two's complement integer.

Proof. Let $D = 0$. Negating any unsigned m -bit integer $\ell \in \mathbb{N}_0$ yields $2^m - 1 - \ell$ (used as statement ‘a’ in the subsequent derivation). It follows

$$(-c - 1) + 1 = -c \quad (18)$$

$$= - \left(-2^{r+1} + 1 + \sum_{i=0}^{r-1} \mathcal{C}_i 2^i \right) \quad (19)$$

$$= 2^{r+1} - 1 - \sum_{i=0}^{r-1} \mathcal{C}_i 2^i \quad (20)$$

$$\stackrel{a}{=} 2^{r+1} - 1 - \left(2^r - 1 - \sum_{i=0}^{r-1} \overline{\mathcal{C}}_i 2^i \right) \quad (21)$$

$$= 2^r + \sum_{i=0}^{r-1} \overline{\mathcal{C}}_i 2^i. \quad (22)$$

Let $D = 1$. Then it holds

$$c + 1 = 2^r - 1 + \left(\sum_{i=0}^{r-1} \mathcal{C}_i 2^i \right) + 1 = 2^r + \sum_{i=0}^{r-1} \mathcal{C}_i 2^i. \quad (23)$$

As both cases yield the desired results we have proven what was to be shown. \square

Refer to [8, rtl/encoder/postencoder.vhd, lines 109–117] for the VHDL implementation of the characteristic precursor determination. As can be observed, only the 8 least significant bits of the characteristic are negated. This approach stems from the fact that the normalised characteristic, by construction, always has a zero in the most significant bit. Consequently, the subsequent incrementation is performed on a ‘standard-form’ 8-bit bit string. It is important to note that employing the precursor enables us to circumvent a potentially necessary decrementation (see Definition 1), while the incrementation can be efficiently implemented using only half-adders.

However, it is crucial to bear in mind that the characteristic bits will need to be negated at a later stage. This step cannot be undertaken at the current moment, as the regime value r has not yet been extracted.

5.3 8-Bit Leading One Detector (LOD)

By construction, the characteristic precursor, represented as an 8-bit unsigned integer, has its most significant set bit always at offset r (see Proposition 2), where r denotes the regime. To determine the regime, it is necessary to employ an 8-bit leading one detector (LOD). We adopt the design proposed in [4], which divides the 8-bit number into two 4-bit segments. Each segment is then processed

through a lookup table, which yields the offset value of the most significant bit set to 1, namely the desired regime value r .

If the most significant four bits are all zero, the result from the lower bits' lookup table is returned. Conversely, if any of the highest four bits are set to 1, the result from the higher bits' lookup table is returned, with 4 added to account for the fact that the leading one inherently has an offset of 4 due to its position. This adjustment ensures accurate determination of the regime. For a detailed implementation, refer to [8, rtl/encoder/postencoder.vhd, lines 119–155].

5.4 Extended Takum Generator

Given the tapered-precision nature of takums, the number of mantissa bits varies; without loss of generality, for $n > 12$ it lies between $n - 12$ and $n - 5$. The encoder input for the mantissa bits has a fixed size of $n - 5$ (and is non-existent for $n < 5$). However, a regime value of 7 implies that the actual mantissa bit count in the output is $n - 12$, not $n - 5$.

Rounding the mantissa bits at this stage is not advisable, since rounding also occurs in the non-mantissa bits and may introduce carry bits originating from the mantissa rounding that would need to be preserved for later non-mantissa rounding. Instead, we construct an ‘extended takum’ of precision $n + 7$, which fully accommodates a mantissa of length $n - 5$ even in the case where there are 7 characteristic bits. This extended takum can then be correctly rounded to n bits in the separate rounder.

The initial step in generating the extended takum involves deriving the regime bits from the regime. According to the definition, this process entails examining the direction bit. As detailed in Section 5.2, the characteristic precursor must also be inverted to obtain the coded characteristic bits, which occurs during the direction bit check.

Upon inverting the characteristic precursor, the resulting characteristic bits are contained within the lower 7 bits of the output. Given that the characteristic bits vary in length from 0 to 7, there will be unused bits in the upper $7 - \text{regime}$ bits. This is not problematic, as we subsequently combine these bits with the mantissa bits and 7 zero bits, then shift the entire sequence *regime* bits to the right. This ensures that the characteristic bits always start at index $n + 1$ and are followed by the mantissa bits, as intended.

We discard the highest 7 bits of the shifted characteristic and mantissa bits, yielding a bit string of length $n + 2$. Considering that the sign bit, direction bit, and three regime bits together occupy a total of 5 bits, the combination of these with the previous bit string forms the $(n + 7)$ -bit extended takum [8, rtl/encoder/postencoder.vhd, lines 157–176].

It is noteworthy that the shifter, regardless of n , is constrained by a maximum shift offset of 7 (three control bits). This contrasts sharply with posits, where the tapering is unbounded and a shifter must accommodate nearly the entire width n .

5.5 Rounder

Having determined whether rounding up or down results in an overflow or underflow (see Section 5.1), and having obtained the $(n + 7)$ -bit extended takum (see Section 5.4), we can now proceed to combine these elements to achieve a properly rounded n -bit takum.

The initial step involves generating two rounding candidates: one for rounding up and one for rounding down. They are obtained by discarding the extended takum's 7 least significant bits, yielding the rounding-down candidate, and incrementing it to yield the rounding-up candidate. The final result is determined by rounding up if either: (1) rounding down would cause an underflow; or (2) rounding up would not cause an overflow, the most significant rounding bit in the extended takum is set and there is either no tie or we are tied and the rounding-down candidate is odd (as we tie to even). If these conditions are not met, we opt for the rounding-down candidate.

This approach is preferred over directly incrementing the takum with the rounding bit by the result of the logic expression, as it optimises timing: while we can immediately start incrementing and determining whether to round up or down as soon as the input arrives, direct incrementing would require waiting for the logic expression to evaluate before beginning the computation [8, rtl/encoder/postencoder.vhd, lines 178–190].

5.6 Post-, Logarithmic and Linear Encoder

With all components in place, we can now integrate them into a single comprehensive component: the postencoder. It is made up of five main entities: the underflow/overflow predictor (E1), the characteristic precursor determinator (E2), the extended takum generator (E3), the rounder (E4) and the output driver (E5). The determination of the direction bit at the outset is given separately, as it is simply the inverted sign bit of the characteristic [8, rtl/encoder/postencoder.vhd]. A full logic circuit is outlined in Figure 2.

For encoding logarithmic takum values, as outlined in [8, rtl/encoder/encoder_logarithmic.vhd], the characteristic and mantissa bits derived from the barred logarithmic value, as defined in (10), are passed into the postencoder. Similarly, the linear takum encoder, as described in [8, rtl/encoder/encoder_linear.vhd], employs the postencoder following the conversion of the internal representation from equation (8). The characteristic is computed from the exponent, with conditional negation applied based on S .

6 Evaluation

Having devised decoders and encoders for both logarithmic and linear takums, we now proceed to evaluate their performance relative to the most effective posit codecs. The synthesis was conducted using Vivado 2024.1 on a Kintex UltraScale+ KCU116 Evaluation Platform (FPGA part number XCKU5P-2FFVB676E) with

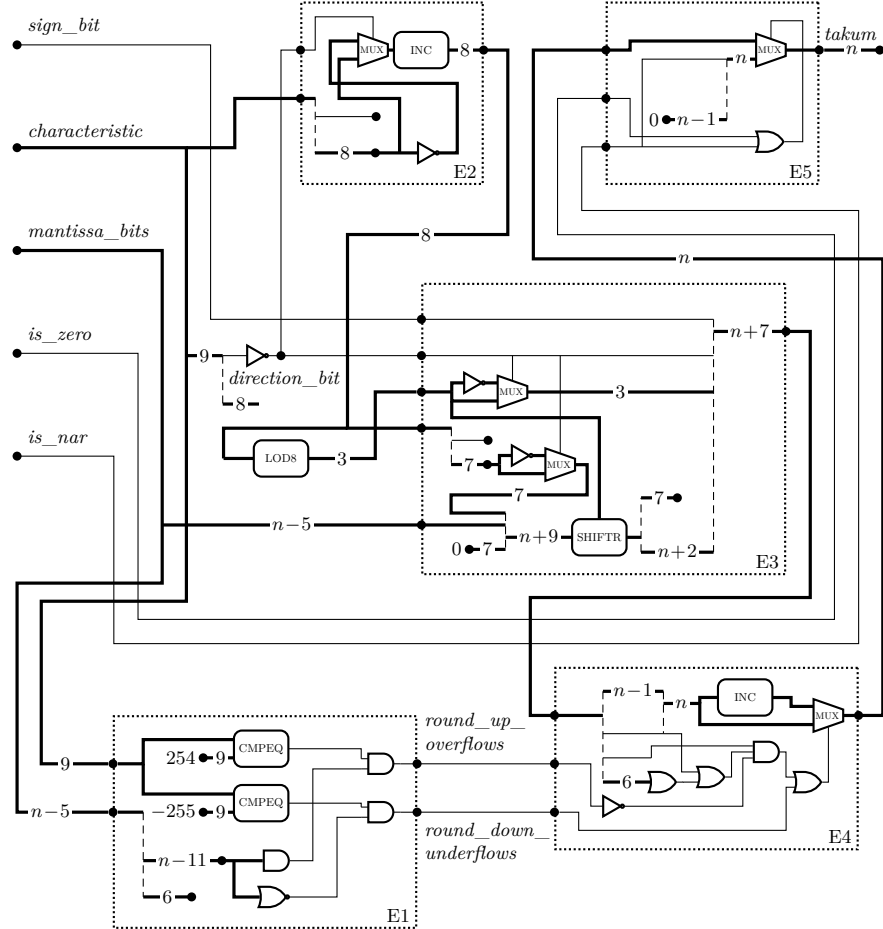


Figure 2: The logic circuit of the postencoder, largely separated into five main entities: the underflow/overflow predictor (E1), the characteristic precursor determinator (E2), the extended takum generator (E3), the rounder (E4) and the output driver (E5). We assume $n \geq 12$ (thus omitting special case handling in the underflow/overflow predictor for $n < 12$) for simplicity; the implemented postencoder works for any $n \geq 2$. Vertical dashed lines indicate where the strands of a multi-signal are split up or combined.

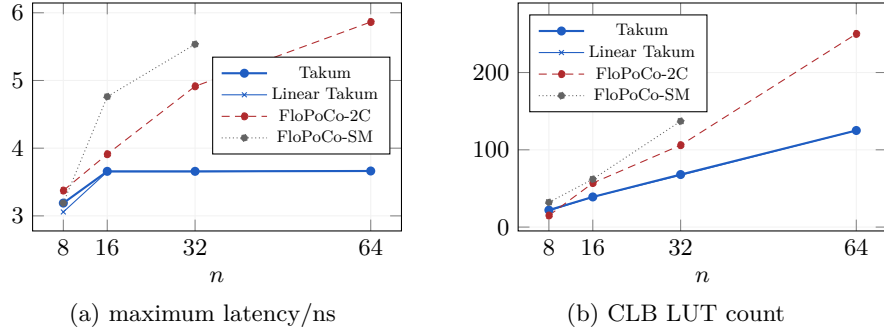


Figure 3: Evaluation results for the decoder in terms of latency and LUT consumption.

a maximum operating frequency of 725 MHz [10]. We employed the default synthesis strategy (Vivado Synthesis Defaults, 2024).

First, both the encoder and decoder are validated using a testbench (see [8, simulation/decoder/predecoder_tb.vhd, simulation/encoder/postencoder_tb.vhd]). While the decoder is verified against a reference implementation, the encoder is assessed through a round-trip test, employing the validated decoder as the initial stage. This procedure ensures the correct operation of both components.

Our takum codec is compared against the sign-magnitude FloPoCo codec ('FloPoCo-SM', see [14, 16, 15]), which utilizes the internal representation detailed in (7), and the enhanced two's complement FloPoCo codec ('FloPoCo-2C') [13], which employs the optimised internal representation described in (8) and is integrated into the PERCIVAL RISC-V core project [12, 11]. For a comparison of the internal representations, refer to Section 3.

The PACoGen codec [9] has been excluded from this comparison due to [13, Figure 7] indicating that its performance is generally inferior or at best comparable to that of the FloPoCo-2C codec. Similarly, the MArTo codec [18] was not included for the same reason. The posit codecs used in this evaluation have been extracted and incorporated into [8, rtl/third_party/].

6.1 Decoder

We begin by assessing the decoder's performance by measuring its maximum latency and look-up table (LUT) consumption on the reference FPGA. With respect to maximum latency, as illustrated in Figure 3a, it is noteworthy that our results for both FloPoCo-SM and FloPoCo-2C are consistent with those reported in [13], despite the use of a different FPGA platform.

The results indicate that the takum decoders outperform both reference decoders, even for $n = 8$ where FloPoCo-SM beats FloPoCo-2C. Overall, the takum decoders' latencies are up to 38 % lower than FloPoCo-2C's. For decoder widths

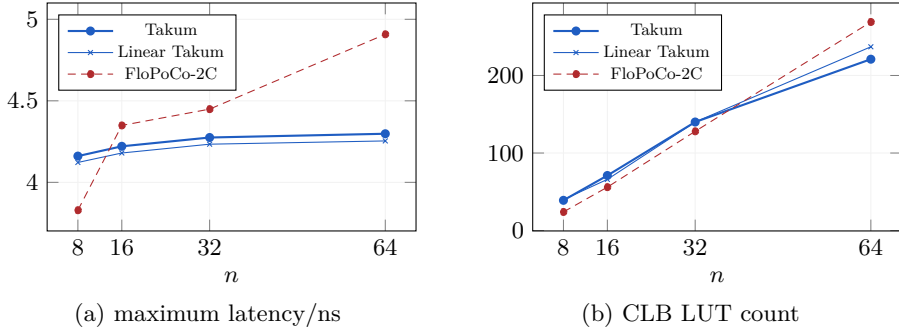


Figure 4: Evaluation results for the encoder in terms of latency and LUT consumption.

ranging from 8 to 64 bits, the FloPoCo-2C decoders can operate at frequencies of up to approximately 170 MHz, whereas the takum decoders achieve up to approximately 270 MHz.

A similar trend is observed in the LUT consumption, as shown in Figure 3b. For $n = 8$, all implementations exhibit comparable LUT usage and nearly linear delay growth. However, the takum decoder demonstrates a significantly lower CLB LUT consumption, with up to 50 % less usage compared to the most efficient posit reference.

6.2 Encoder

In our comparison of encoders it is important to note that FloPoCo-SM is not included. This omission is due to the fact that FloPoCo-SM lacks a distinct posit encoder within its codebase that could be evaluated separately. Instead, the posit encoder is integrated with the arithmetic logic in FloPoCo-SM. This poses no issue, as FloPoCo-2C, its superior successor, provides distinct decoders and encoders.

Additionally, while the takum encoder incorporates comprehensive rounding logic, the FloPoCo-2C encoder does not and depends on external rounding information provided by the caller, which must be determined beforehand and limits the posit encoder's usability. Within the scope of this comparison, the proposed takum encoder is consequently at a significant disadvantage, as it has to derive this rounding information on its own.

Moreover, for $n = 16$, the synthesiser defaults to using LUTs instead of a CARRY8 chain for computing *takum_rounded_up*, increasing the delay. To address this, synthesis settings were adjusted to enforce the use of a CARRY8 chain. The same approach was taken with the linear and logarithmic takum encoders to enforce consistent synthesis for $n = 8$.

An examination of the maximum latency presented in Figure 4a reveals that, although the takum encoders exhibit higher latency for $n = 8$, their latencies increase only marginally as n grows, ultimately being up to 13% lower than those of the FloPoCo-2C encoder. In contrast, the latency of the (non-rounding) FloPoCo-2C encoder increases more significantly with larger values of n . Both the logarithmic and linear variants of the takum encoder display comparable performance characteristics across the range of n . For encoder widths ranging from 8 to 64 bits, the FloPoCo-2C encoders can operate at frequencies of up to approximately 200 MHz, whereas the takum encoders achieve up to approximately 230 MHz.

In terms of slice LUT consumption, as illustrated in Figure 4b, the takum and posit encoders show comparable usage. The non-rounding FloPoCo-2C encoder exhibits a slight advantage for $n \leq 32$, whereas the takum encoders have an advantage for $n = 64$.

7 Conclusion and Outlook

We have demonstrated the design and implementation of a takum hardware codec using VHDL, proposing a new internal LNS representation for improved performance. Our evaluations reveal that the takum codec significantly outperforms the leading posit codec, FloPoCo-2C, while not relying on outside rounding information at the encoding stage, and demonstrates near-optimal scalability with respect to n . This superior performance can largely be attributed to the fact that the coded exponent in takums is bounded, whereas for posits it is unbounded, and the use of elegant transforms made possible by it. In contrast, posits require logic that encompasses the entire width of the binary string, spanning all bits during both decoding and encoding operations (for instance, shifts), rather than just the initial 12 bits. Therefore, takums can be said to be generally more hardware-efficient compared to posits on FPGA platforms, at least in regard to the codec design, since the full design of an arithmetic processing unit (APU) introduces additional variables. Nevertheless, given that posits and takums share the same internal representation, the codec largely remains the sole distinguishing component.

Future work will evaluate the performance of the takum codec on VLSI systems, given that the complexity of FPGA implementations does not always correlate with VLSI complexity. Another aspect concerns the evaluation of the codec implemented within a full APU, potentially as a pipelined design, in direct comparison with the current state of the art in IEEE 754 APUs. An additional task would be discussing the implementation of the ‘quire’ accumulator, as used in posit arithmetic. Furthermore, it is warranted to investigate the effects of the novel choice of base \sqrt{e} in (logarithmic) takums on the hardware implementation of an arithmetic core. This aspect is tentatively addressed in [7, Section 4.4]. However, a comprehensive hardware implementation is necessary for a thorough assessment.

References

- [1] Zachariah Carmichael et al. ‘Deep Positron: A Deep Neural Network Using the Posit Number System’. In: *2019 Design, Automation & Test in Europe Conference & Exhibition (DATE)*. 2019, pp. 1421–1426. DOI: [10.23919/DATE.2019.8715262](https://doi.org/10.23919/DATE.2019.8715262).
- [2] Rohit Chaurasiya et al. ‘Parameterized Posit Arithmetic Hardware Generator’. In: *2018 IEEE 36th International Conference on Computer Design (ICCD)*. 2018, pp. 334–341. DOI: [10.1109/ICCD.2018.00057](https://doi.org/10.1109/ICCD.2018.00057).
- [3] Florent de Dinechin et al. ‘Posits: The Good, the Bad and the Ugly’. In: CoNGA’19. Singapore, Singapore: Association for Computing Machinery, 2019. DOI: [10.1145/3316279.3316285](https://doi.org/10.1145/3316279.3316285).
- [4] Zahra Ebrahimi et al. ‘Plasticine: A Cross-layer Approximation Methodology for Multi-kernel Applications through Minimally Biased, High-throughput, and Energy-efficient SIMD Soft Multiplier-divider’. In: *ACM Transactions on Design Automation of Electronic Systems (TODAES)* 27.2 (Nov. 2021). DOI: [10.1145/3486616](https://doi.org/10.1145/3486616).
- [5] John L. Gustafson and Isaac Yonemoto. ‘Beating Floating Point at Its Own Game: Posit Arithmetic’. In: *Supercomputing Frontiers and Innovations* 4.2 (June 2017), pp. 71–86. DOI: [10.14529/jsfi170206](https://doi.org/10.14529/jsfi170206).
- [6] John L. Gustafson et al. ‘Standard for Posit™ Arithmetic’. Mar. 2022. URL: https://web.archive.org/web/20220603115338/https://posithub.org/docs/posit_standard-2.pdf.
- [7] Laslo Hunhold. ‘Beating Posits at Their Own Game: Takum Arithmetic’. In: *Next Generation Arithmetic. 5th International Conference, CoNGA 2024, Sydney, NSW, Australia, February 20–21, 2024, Proceedings*. Vol. 14666. Lecture Notes in Computer Science. Sydney, NSW, Australia: Springer Nature Switzerland, Oct. 2024. DOI: [10.1007/978-3-031-72709-2_1](https://doi.org/10.1007/978-3-031-72709-2_1).
- [8] Laslo Hunhold. *Takum Codec RTL*. Version v1.1.0. Aug. 2025. DOI: [10.5281/zenodo.16923066](https://doi.org/10.5281/zenodo.16923066).
- [9] Manish Kumar Jaiswal and Hayden K.-H. So. ‘PACoGen: A Hardware Posit Arithmetic Core Generator’. In: *IEEE Access* 7 (2019), pp. 74586–74601. DOI: [10.1109/ACCESS.2019.2920936](https://doi.org/10.1109/ACCESS.2019.2920936).
- [10] *Kintex UltraScale+ FPGAs Data Sheet: DC and AC Switching Characteristics (DS922)*. Version 1.18. Advanced Micro Devices, Inc. (AMD). Aug. 2024. 74 pp. URL: <https://web.archive.org/web/20250927173543/https://docs.amd.com/api/khub/maps/PukeDYQrenc50UQpPyCC3A/attachments/fQq1e3qru~eHvPovjuU79g-PukeDYQrenc50UQpPyCC3A/content>.
- [11] David Mallasén et al. ‘Big-PERCIVAL: Exploring the Native Use of 64-Bit Posit Arithmetic in Scientific Computing’. In: *IEEE Transactions on Computers* 73.6 (June 2024), pp. 1472–1485. DOI: [10.1109/TC.2024.3377890](https://doi.org/10.1109/TC.2024.3377890).

- [12] David Mallasén et al. ‘PERCIVAL: Open-Source Posit RISC-V Core With Quire Capability’. In: *IEEE Transactions on Emerging Topics in Computing* 10.3 (2022), pp. 1241–1252. DOI: 10.1109/TETC.2022.3187199.
- [13] Raul Murillo et al. ‘Comparing Different Decodings for Posit Arithmetic’. In: *Conference on Next Generation Arithmetic*. Springer. 2022, pp. 84–99. DOI: 10.1007/978-3-031-09779-9_6.
- [14] Raul Murillo et al. ‘Customized Posit Adders and Multipliers Using the FloPoCo Core Generator’. In: *2020 IEEE International Symposium on Circuits and Systems (ISCAS)*. IEEE. 2020, pp. 1–5. DOI: 10.1109/ISCAS45731.2020.9180771.
- [15] Raul Murillo et al. ‘Energy-Efficient MAC Units for Fused Posit Arithmetic’. In: *2021 IEEE 39th International Conference on Computer Design (ICCD)*. IEEE. 2021, pp. 138–145. DOI: 10.1109/ICCD53106.2021.00032.
- [16] Raul Murillo et al. ‘PLAM: a Posit Logarithm-Approximate Multiplier’. In: *IEEE Transactions on Emerging Topics in Computing* (2021), pp. 2079–2085. DOI: 10.1109/TETC.2021.3109127.
- [17] Akshat Ramachandran et al. ‘Algorithm-Hardware Co-Design of Distribution-Aware Logarithmic-PoSit Encodings for Efficient DNN Inference’. In: (Mar. 2024), pp. 1–6. arXiv: 2403.05465 [cs.HA].
- [18] Yohann Uguen et al. ‘Evaluating the Hardware Cost of the Posit Number System’. In: *2019 29th International Conference on Field Programmable Logic and Applications (FPL)*. 2019, pp. 106–113. DOI: 10.1109/FPL.2019.00026.
- [19] Shibo Wang and Pankaj Kanwar. ‘BFLOAT16: The Secret to High Performance on Cloud TPUs’. Aug. 2019. URL: <https://web.archive.org/web/20190826170119/https://cloud.google.com/blog/products/ai-machine-learning/bfloat16-the-secret-to-high-performance-on-cloud-tpus>.